JOURNAL OF CIVIL ENGINEERING AND MANAGEMENT
2009
15(1): 35–46

HILLTOP BUCKLING AS THE A AND Ω IN SENSITIVITY ANALYSIS OF THE INITIAL POSTBUCKLING BEHAVIOR OF ELASTIC STRUCTURES

Herbert A. Mang[1], Xin Jia[2], Gerhard Hoefinger[3]

Institute for Mechanics of Materials and Structures, Vienna University of Technology,
Karlsplatz 13/202, 1040 Vienna, Austria, e-mail: [1]herbert.mang@tuwien.ac.at

Received 22 Aug 2008, accepted 23 Jan 2009

Abstract. The coincidence of a bifurcation point with a snap-through point is called hilltop buckling. In this paper, it either serves as the starting point – the A – or as the end – the Ω – in sensitivity analysis of the initial postbuckling behavior of elastic structures. It is shown that hilltop buckling is imperfection sensitive. In sensitivity analyses with hilltop buckling as the starting point (end), the bifurcation point and the snap-through point are diverging from (converging to) each other. Two classes of sensitivity analyses are identified by means of the consistently linearized eigenproblem. They determine the more (or less) effective mode of conversion of an originally imperfection-sensitive into an imperfection-insensitive structure. The results from the numerical investigation corroborate the theoretical findings. The present study is viewed as a step in the direction of better understanding the reasons for different modes of the initial postbuckling behavior of elastic structures and its interplay with the prebuckling behavior.

Keywords: consistently linearized eigenproblem, hilltop buckling, imperfection (in)sensitivity, Koiter's initial postbuckling analysis, sensitivity analysis, symmetric bifurcation, zero-stiffness postbuckling.

1. Introduction

The coincidence of a bifurcation point with a snap-through point is called hilltop buckling (Fujii, Nogushi 2002). It can be realized by appropriately tuning a set of design parameters of a structure (Steinboeck *et al.* 2008a).

Assuming that hilltop buckling is imperfection sensitive, it may serve as the starting point – the Alpha – for sensitivity analysis of the buckling load and the initial postbuckling behavior by means of variation of a design parameter. The motivation for such an analysis may be improvement of this behavior through conversion of an originally imperfection-sensitive into an imperfection-insensitive structure (Mang *et al.* 2006; Schranz *et al.* 2006). In the course of this analysis, the stability limit, represented by the bifurcation point, is increasing less strongly than the load corresponding to the snap-through point. Hence, the two points are diverging from each other.

Conversely, in sensitivity analysis the stability limit may be increasing more strongly than the snap-through load. In this case, the two load points are converging to each other. Their coincidence represents the end – the Omega – of sensitivity analysis of the buckling load and the initial postbuckling behavior because snap-through would otherwise replace bifurcation buckling as the relevant mode of loss of stability.

The purpose of this paper is to examine these two forms of sensitivity analyses of the buckling load and the initial postbuckling behavior. Examination tools include Koiter's initial postbuckling analysis (Koiter 1967) and the Finite Element Method (FEM).

It will be shown that hilltop buckling is imperfection sensitive. As a special form of transition from imperfection sensitivity to imperfection insensitivity, zero- stiffness postbuckling (Steinboeck *et al.* 2008b) will be mentioned.

The investigation is restricted to static, conservative, perfect systems with a finite number N of degrees of freedom as conforms to the FEM. The material behavior is assumed to be either rigid or linear elastic. Only symmetric bifurcation behavior with respect to a scalar variable η will be considered (Steinboeck *et al.* 2008b). Multiple bifurcation will be excluded, especially multiple hilltop buckling will not be discussed in this analysis, i.e. there is only one single secondary path will be considered. For a discussion on multiple hilltop branching phenomena and their influence on imperfection sensitivity refer to (Fujii, Noguchi 2002; Ohsaki, Ikeda 2006). The numerical results of examples presented there corroborate the following theoretical findings. Sensitivity analysis will be restricted to variation of one design parameter at a time.

2. Derivation of polynomials

2.1. Koiter's initial postbuckling analysis

Fig. 1 shows a projection of load-displacement paths of a system bifurcating at point C. The solid line represents the *primary* path, whereas the dashed line is a *secondary* path. The latter is parameterized by $\eta \in \mathbb{R}$, defined as

ISSN 1392–3730 print / ISSN 1822–3605 online
DOI: 10.3846/1392-3730.2009.15.35-46

zero at C. Herein, the subscript $\bullet_C$ means evaluation of a quantity at C. The reference load $\bar{\boldsymbol{P}}$ is scaled by a dimensionless load factor λ, and $\boldsymbol{u}$ denotes the vector of generalized displacement coordinates.

In Mang, Schranz (2006) and Steinboeck *et al.* (2008b) Koiter's initial postbuckling analysis (Koiter 1967) was used to expand the out-of-balance force

$$\boldsymbol{G}(\boldsymbol{u},\lambda) := \boldsymbol{F}^{\boldsymbol{I}}(\boldsymbol{u}) - \lambda\bar{\boldsymbol{P}} \in \mathbb{R}^N, \tag{1}$$

where $\boldsymbol{F}^{\boldsymbol{I}}(\boldsymbol{u})$ denotes the internal forces, into an asymptotic series at C. For a static, conservative system, $\boldsymbol{G}$ can be derived from the potential energy function V as

$$\boldsymbol{G} = \frac{\partial V}{\partial \boldsymbol{u}}. \tag{2}$$

$\boldsymbol{G}$ vanishes along equilibrium paths in the $\boldsymbol{u}-\lambda$ space. $\lambda(\eta)$ is the load level at the point of the secondary path associated with η, as outlined in Fig. 1. The point on the primary path characterized by the same load is described by the displacement vector $\tilde{\boldsymbol{u}}(\lambda(\eta))$. Quantities evaluated along the primary path are labeled by an upper tilde. The displacement at the corresponding point of the secondary path can be expressed as $\boldsymbol{u}(\eta) = \tilde{\boldsymbol{u}}(\lambda(\eta)) + \boldsymbol{v}(\eta)$ where $\boldsymbol{v}$ is the displacement offset which vanishes trivially at C. Hence,

$$\boldsymbol{G}(\eta) := \boldsymbol{G}(\tilde{\boldsymbol{u}}(\lambda(\eta)) + \boldsymbol{v}(\eta), \lambda(\eta)) = \boldsymbol{0} \tag{3}$$

must hold along the secondary path. Insertion of the asymptotic series expansions

$$\lambda(\eta) = \lambda_C + \lambda_1\eta + \lambda_2\eta^2 + \lambda_3\eta^3 + O(\eta^4), \tag{4}$$

$$\boldsymbol{v}(\eta) = \boldsymbol{v}_1\eta + \boldsymbol{v}_2\eta^2 + \boldsymbol{v}_3\eta^3 + O(\eta^4) \tag{5}$$

into (3) and expanding the resulting expressions into a series in terms of η yields

$$\boldsymbol{G} = \boldsymbol{G}_{0C} + \boldsymbol{G}_{1C}\eta + \boldsymbol{G}_{2C}\eta^2 + \boldsymbol{G}_{3C}\eta^3 + O(\eta^4) \tag{6}$$

with

$$\boldsymbol{G}_{nC} = \frac{\boldsymbol{G}_{,\eta^n C}}{n!} \quad \forall\ n \in \mathbb{N}, \tag{7}$$

where $\mathbb{N}$ denotes the set of natural numbers including zero. Details of computation of $\boldsymbol{G}_{nC}$ are given in (Steinboeck *et al.* 2008b).

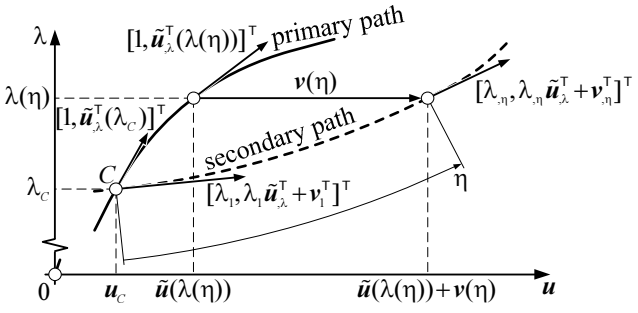

Fig. 1. On Koiter's initial postbuckling analysis (Steinboeck *et al.* 2008)

Since (3) must hold for any point along the secondary path, i.e. for arbitrary values of η, each coefficient $\boldsymbol{G}_{nC}$ of the series must vanish. This condition paves the way for successive calculation of the pairs of unknowns $(\boldsymbol{v}_1, \lambda_1)$, $(\boldsymbol{v}_2, \lambda_2)$, etc. described in (Mang, Schranz 2006).

2.2. Coefficients of the asymptotic series expansion of $\lambda(\eta) - \lambda_C$

For the present investigation only the first four coefficients of the series expansion of $\lambda(\eta)$ need to be known. They are given as follows (Mang, Schranz 2006):

$$\lambda_1 = d_0, \tag{8}$$

$$\lambda_2 = a_1\lambda_1^2 + b_1\lambda_1 + d_1, \tag{9}$$

$$\lambda_3 = a_1^*\lambda_1^3 + b_1^*\lambda_1^2 + c_1^*\lambda_1 + b_1\lambda_2 + d_2, \tag{10}$$

$$\lambda_4 = \hat{a}_1\lambda_1^4 + \hat{b}_1\lambda_1^3 + \hat{c}_1\lambda_1^2 + \hat{d}_1\lambda_1 + a_1\lambda_2^2 + b_2\lambda_2 + b_1\lambda_3 + d_3, \tag{11}$$

where

$$c_1^* = 2a_1\lambda_2 + b_2, \tag{12}$$

$$\hat{c}_1 = 3a_1^*\lambda_2 + \frac{1}{2}b_2^*, \tag{13}$$

$$\hat{d}_1 = 2b_1^*\lambda_2 + 2a_1\lambda_3 + b_3, \tag{14}$$

whereas none of the other coefficients in the expressions for λ_3 and λ_4 depends on λ_2, and λ_2 and λ_3, respectively.

To get an idea of the structure of the coefficients in (8)–(11), the expressions for d_0 (b_0 in (Mang *et al.* 2006), a_1, b_1, d_1, and a_1^* are listed in the following (Mang, Schranz 2006):

$$d_0 = -\frac{1}{2}\frac{\boldsymbol{v}_1^T \cdot \boldsymbol{K}_{T,u} : \boldsymbol{v}_1 \otimes \boldsymbol{v}_1}{\boldsymbol{v}_1^T \cdot \tilde{\boldsymbol{K}}_{T,\lambda} \cdot \boldsymbol{v}_1}, \tag{15}$$

$$a_1 = -\frac{1}{2}\frac{\boldsymbol{v}_1^T \cdot \tilde{\boldsymbol{K}}_{T,\lambda\lambda} \cdot \boldsymbol{v}_1}{\boldsymbol{v}_1^T \cdot \tilde{\boldsymbol{K}}_{T,\lambda} \cdot \boldsymbol{v}_1}, \tag{16}$$

$$b_1 = -\frac{\boldsymbol{v}_1^T \cdot \tilde{\boldsymbol{K}}_{T,\lambda} \cdot \boldsymbol{v}_2 + \frac{1}{2}\boldsymbol{v}_1^T \cdot \boldsymbol{K}_{T,u\lambda} : \boldsymbol{v}_1 \otimes \boldsymbol{v}_1}{\boldsymbol{v}_1^T \cdot \tilde{\boldsymbol{K}}_{T,\lambda} \cdot \boldsymbol{v}_1}, \tag{17}$$

$$d_1 = -\frac{\boldsymbol{v}_1^T \cdot \boldsymbol{K}_{T,u} : \boldsymbol{v}_1 \otimes v_2 + \frac{1}{6}\boldsymbol{v}_1^T \cdot \boldsymbol{K}_{T,uu} \vdots \boldsymbol{v}_1 \otimes \boldsymbol{v}_1 \otimes \boldsymbol{v}_1}{\boldsymbol{v}_1^T \cdot \tilde{\boldsymbol{K}}_{T,\lambda} \cdot \boldsymbol{v}_1}, \tag{18}$$

$$a_1^* = -\frac{1}{6}\frac{\boldsymbol{v}_1^T \cdot \tilde{\boldsymbol{K}}_{T,\lambda\lambda\lambda} \cdot \boldsymbol{v}_1}{\boldsymbol{v}_1^T \cdot \tilde{\boldsymbol{K}}_{T,\lambda} \cdot \boldsymbol{v}_1}. \tag{19}$$

$\boldsymbol{K}_T(\boldsymbol{u}) = \boldsymbol{G}_{,u}$ is the tangent stiffness matrix which generally refers to out-of-balance states, whereas

$$\tilde{\boldsymbol{K}}_T(\lambda) := \boldsymbol{K}_T(\tilde{\boldsymbol{u}}(\lambda)) \tag{20}$$

is the one that refers to the special case of equilibrium states on the primary path. $(\bullet)_{,\lambda}$ indicates the special differentiation with respect to λ along a direction parallel

to the primary path (Mang, Schranz 2006). Most of the coefficients in (8)–(11) are given in (Mang, Schranz 2006). The remaining coefficients can be deduced from Appendix B in (Mang, Schranz 2006).

3. Specialization of the expressions for $\lambda_1,\ldots,\lambda_4$ for symmetric bifurcation

3.1. Conditions for symmetric bifurcation

Bifurcation is qualified as *symmetric* with respect to the parameter η if it obeys the definitions (Steinboeck *et al.* 2008b):

$$\lambda(\eta)=\lambda(-\eta)\wedge \tag{21}$$

$$\boldsymbol{v}(\eta)=T\left(\boldsymbol{v}(-\eta)\right)\wedge \tag{22}$$

$$\tilde{\boldsymbol{u}}\left(\lambda(\eta)\right)=T\left(\tilde{\boldsymbol{u}}\left(\lambda(\eta)\right)\right), \tag{23}$$

where the linear mapping $T:\mathbb{R}^N\to\mathbb{R}^N$ is an element of a symmetry group. Insertion of (4) into (21) yields

$$\lambda_1=\lambda_3=....=0\,. \tag{24}$$

3.2. Specialization of (8)–(11) for symmetric bifurcation

Substitution of (24) into (8)–(11) gives

$$0=d_0\,, \tag{25}$$

$$\lambda_2=d_1\,, \tag{26}$$

$$0=b_1\lambda_2+d_2\,, \tag{27}$$

$$\lambda_4=a_1\lambda_2^2+b_2\lambda_2+d_3\,. \tag{28}$$

According to (Steinboeck *et al.* 2008b), symmetric bifurcation requires

$$d_0=d_2=....=0. \tag{29}$$

Hence, following from (27),

$$b_1=0. \tag{30}$$

This corresponds with the result of a proof in (Steinboeck *et al.* 2008b) according to which b_1, b_1^*, $\hat{b}_1$, …, $\hat{d}_1$, … must vanish for symmetric bifurcation. Hence, following from (14), also

$$b_3=0. \tag{31}$$

4. Conditions for imperfection insensitivity

A necessary condition for imperfection insensitivity is given as (Bochenek 2003)

$$\lambda_1=0\,, \tag{32}$$

which is automatically satisfied for symmetric bifurcation. Sufficient conditions for imperfection sensitivity are (Bochenek 2003):

$$\lambda_1=0,\ \lambda_2>0. \tag{33}$$

Hence, symmetric bifurcation is not necessary for imperfection insensitivity (Helnwein 1997). If $\lambda_1=0\wedge\lambda_2=0$,

$$\lambda_3=0 \tag{34}$$

is a necessary condition for imperfection insensitivity which is automatically satisfied for symmetric bifurcation. Sufficient conditions for imperfection insensitivity in this case are

$$\lambda_3=0,\ \lambda_4>0. \tag{35}$$

Thus, for imperfection insensitivity the first non-vanishing coefficient in the asymptotic series expansion (4) must have an even subscript which is automatically the case for symmetric bifurcation, and must be positive.

5. Hilltop buckling

In the following it will be proved that hilltop buckling is imperfection sensitive. Introducing the parameter ξ, which refers to the primary path, into (16), gives

$$a_1=-\frac{1}{2\lambda_{,\xi}}\left(\frac{\boldsymbol{v}_1^T\cdot\tilde{\boldsymbol{K}}_{T,\xi\xi}\cdot\boldsymbol{v}_1}{\boldsymbol{v}_1^T\cdot\tilde{\boldsymbol{K}}_{T,\xi}\cdot\boldsymbol{v}_1}-\frac{\lambda_{,\xi\xi}}{\lambda_{,\xi}}\right)\Bigg|_{\xi=\xi_C}, \tag{36}$$

with $\xi=\xi_C$ indicating the stability limit $\lambda=\lambda_C$.

At the snap-through point, $\lambda(\xi)$ has a local maximum:

$$\lambda_{,\xi}=0,\ \lambda_{,\xi\xi}<0\,. \tag{37}$$

Because of

$$\boldsymbol{v}_1^T\cdot\tilde{\boldsymbol{K}}_{T,\xi}\cdot\boldsymbol{v}_1\neq 0,\ \left|\boldsymbol{v}_1^T\cdot\tilde{\boldsymbol{K}}_{T,\xi\xi}\cdot\boldsymbol{v}_1\right|\neq\infty, \tag{38}$$

the first term in parentheses of (36) is negligible. Thus

$$a_1=-\infty. \tag{39}$$

Because of $\lambda_{,\xi\xi}\big/\lambda_{,\xi}^2$ with (37), a_1 has a pole of 2nd order.

Alternatively, the path parameter η, referring to the secondary path, is inserted into (16), which gives

$$a_1=-\frac{1}{2\lambda_{,\eta}}\left(\frac{\boldsymbol{v}_1^T\cdot\tilde{\boldsymbol{K}}_{T,\eta\eta}\cdot\boldsymbol{v}_1}{\boldsymbol{v}_1^T\cdot\tilde{\boldsymbol{K}}_{T,\eta}\cdot\boldsymbol{v}_1}-\frac{\lambda_{,\eta\eta}}{\lambda_{,\eta}}\right)\Bigg|_{\eta=0}, \tag{40}$$

with $\eta=0$, indicating the stability limit $\lambda=\lambda_C$.
Equating the right-hand side of (40) to the one of (36) gives

$$\lambda_{,\eta\eta}\big|_{\eta=0}=\left(\frac{\lambda_{,\eta}\big|_{\eta=0}}{\lambda_{,\xi}\big|_{\xi=\xi_C}}\right)^2\lambda_{,\xi\xi}-\left(\frac{\lambda_{,\eta}\big|_{\eta=0}}{\lambda_{,\xi}\big|_{\xi=\xi_C}}\right)^2 \tag{41}$$

$$\left.\frac{\boldsymbol{v}_1^T\cdot\tilde{\boldsymbol{K}}_{T,\xi\xi}\cdot\boldsymbol{v}_1}{\boldsymbol{v}_1^T\cdot\dfrac{\tilde{\boldsymbol{K}}_{T,\xi}}{\lambda_{,\xi}}\cdot\boldsymbol{v}_1}\right|_{\xi=\xi_C}+\left.\frac{\boldsymbol{v}_1^T\cdot\tilde{\boldsymbol{K}}_{T,\eta\eta}\cdot\boldsymbol{v}_1}{\boldsymbol{v}_1^T\cdot\dfrac{\tilde{\boldsymbol{K}}_{T,\eta}}{\lambda_{,\eta}}\cdot\boldsymbol{v}_1}\right|_{\eta=0},\quad \lambda_{,\xi}>0,$$

where, for the time being, hilltop buckling is excluded. Inserting

$$\lambda_{,\eta}\big|_{\eta=0}=\lambda_1\ \text{ and }\ \lambda_{,\eta\eta}\big|_{\eta=0}=2\lambda_2, \tag{42}$$

which follows from (4), and

$$\boldsymbol{v}_1^T\cdot\frac{\tilde{\boldsymbol{K}}_{T,\eta}}{\lambda_{,\eta}}\cdot\boldsymbol{v}_1\Bigg|_{\eta=0}=\boldsymbol{v}_1^T\cdot\frac{\tilde{\boldsymbol{K}}_{T,\xi}}{\lambda_{,\xi}}\cdot\boldsymbol{v}_1\Bigg|_{\xi=\xi_C}=\boldsymbol{v}_1{}^T\cdot\tilde{\boldsymbol{K}}_{T,\lambda}\cdot\boldsymbol{v}_1\big|_{\lambda=\lambda_C} \tag{43}$$

into (41) yields

$$\lambda_2 = \frac{1}{2}\left(\frac{\lambda_1}{\lambda_{,\xi}\big|_{\xi=\xi_C}}\right)^2\left(\lambda_{,\xi\xi}\big|_{\xi=\xi_C} - \frac{\boldsymbol{v}_1^T\cdot\tilde{\boldsymbol{K}}_{T,\xi\xi}\big|_{\xi=\xi_C}\cdot\boldsymbol{v}_1}{\boldsymbol{v}_1^T\cdot\tilde{\boldsymbol{K}}_{T,\lambda}\big|_{\lambda=\lambda_C}\cdot\boldsymbol{v}_1}\right) + \frac{1}{2}\frac{\boldsymbol{v}_1^T\cdot\tilde{\boldsymbol{K}}_{T,\eta\eta}\big|_{\eta=0}\cdot\boldsymbol{v}_1}{\boldsymbol{v}_1^T\cdot\tilde{\boldsymbol{K}}_{T,\lambda}\big|_{\lambda=\lambda_C}\cdot\boldsymbol{v}_1}, \tag{44}$$

where (Mang *et al.* 2006)

$$-\infty < \boldsymbol{v}_1^T\cdot\tilde{\boldsymbol{K}}_{T,\xi}\big|_{\xi=\xi_C}\cdot\boldsymbol{v}_1 < 0. \tag{45}$$

In order not to *a priori* dismiss the antithesis, i.e. the possibility of imperfection insensitivity for hilltop buckling, the special case of

$$\lambda_{,\eta}\big|_{\eta=0} = \lambda_1 = 0 \tag{46}$$

will be considered, resulting in

$$\lambda_2 = \frac{1}{2}\frac{\boldsymbol{v}_1^T\cdot\tilde{\boldsymbol{K}}_{T,\eta\eta}\big|_{\eta=0}\cdot\boldsymbol{v}_1}{\boldsymbol{v}_1^T\cdot\tilde{\boldsymbol{K}}_{T,\lambda}\big|_{\lambda=\lambda_C}\cdot\boldsymbol{v}_1}, \tag{47}$$

where

$$0 \le \left|\boldsymbol{v}_1^T\cdot\tilde{\boldsymbol{K}}_{T,\eta\eta}\cdot\boldsymbol{v}_1\right| < \infty. \tag{48}$$

Following from (45), (47) and (48), $\lambda_2 = 0$ requires

$$\boldsymbol{v}_1^T\cdot\tilde{\boldsymbol{K}}_{T,\eta\eta}\big|_{\eta=0}\cdot\boldsymbol{v}_1 = 0. \tag{49}$$

Extending now the validity of (47) to hilltop buckling, i.e. replacing (41.2) by

$$\lambda_{,\xi} \ge 0, \tag{50}$$

requires extending the range in (45) from $(-\infty, 0)$ to $[-\infty, 0)$ and in (48) from $[0, \infty)$ to $[0, \infty]$. Hence, for hilltop buckling $\lambda_2 = 0$ represents an indeterminate expression with

$$\boldsymbol{v}_1^T\cdot\tilde{\boldsymbol{K}}_{T,\lambda}\big|_{\lambda=\lambda_C}\cdot\boldsymbol{v}_1 = -\infty \quad\wedge\quad \left|\boldsymbol{v}_1^T\cdot\tilde{\boldsymbol{K}}_{T,\eta\eta}\big|_{\eta=0}\cdot\boldsymbol{v}_1\right| = \infty. \tag{51}$$

To show that hilltop buckling is necessarily imperfection sensitive, a design parameter κ is increased. Initially,

$$\kappa = \kappa_0 \ge 0, \quad \lambda_2(\kappa_0) < 0, \quad \lambda_{2,\kappa}(\kappa_0) > 0. \tag{52}$$

The purpose of this sensitivity study is conversion of an originally imperfection sensitive into an imperfection insensitive structure. As follows from (45) and its extension to (51.1), and from (47) and (51.2),

$$0 < \boldsymbol{v}_1^T\cdot\tilde{\boldsymbol{K}}_{T,\eta\eta}\big|_{\eta=0}\cdot\boldsymbol{v}_1\big|_{\kappa=\kappa_0} \le \infty. \tag{53}$$

If hilltop buckling occurs for $\kappa = \kappa_0$,

$$\boldsymbol{v}_1^T\cdot\tilde{\boldsymbol{K}}_{T,\eta\eta}\big|_{\eta=0}\cdot\boldsymbol{v}_1\big|_{\kappa=\kappa_0} = \infty. \tag{54}$$

Fig. 2a refers to this situation. It shows that hilltop buckling is imperfection sensitive.

If hilltop buckling occurs for $\kappa = \kappa_H = \kappa_0$,

$$0 < \boldsymbol{v}_1^T\cdot\tilde{\boldsymbol{K}}_{T,\eta\eta}\big|_{\eta=0}\cdot\boldsymbol{v}_1\big|_{\kappa=\kappa_0} < \infty, \tag{55}$$

$$\boldsymbol{v}_1^T\cdot\tilde{\boldsymbol{K}}_{T,\eta\eta}\big|_{\eta=0}\cdot\boldsymbol{v}_1\big|_{\kappa=\kappa_H} = \infty, \tag{56}$$

(56) follows from the fact that for both cases

$$\left(\boldsymbol{v}_1^T\cdot\tilde{\boldsymbol{K}}_{T,\lambda}\big|_{\lambda=\lambda_C}\cdot\boldsymbol{v}_1\right)_{,\kappa\kappa} < 0, \left(\boldsymbol{v}_1^T\cdot\tilde{\boldsymbol{K}}_{T,\eta\eta}\big|_{\eta=0}\cdot\boldsymbol{v}_1\right)_{,\kappa\kappa} > 0. \tag{57}$$

Fig. 2(b) refers to $\kappa = \kappa_H > \kappa_0$. It shows that also for this case hilltop buckling is imperfection sensitive.

Information about λ_4 is obtained from specialization of (28) for $a_1 = -\infty^2$ and $\lambda_2 < 0$ and consideration of the following scheme:

$$\begin{array}{rcccccc} \lambda_4 & = & a_1\lambda_2^2 & + & d_3 & + & b_2\lambda_2 \\ & & -\infty^2 & + & \infty^2 & & \\ & & & + & \infty^1 & - & \infty^1 \\ & & & & & - & \infty^0. \end{array} \tag{58}$$

In this scheme, "∞^2", "∞^1", and "∞^0" denote a pole of 2nd, 1st, and 0th order (with respect to a variable design parameter κ), noting that the latter is a positive, finite number. The scheme is based on the hypothesis that (58) cannot disintegrate at hilltop buckling. Numerical results have validated the scheme according to which

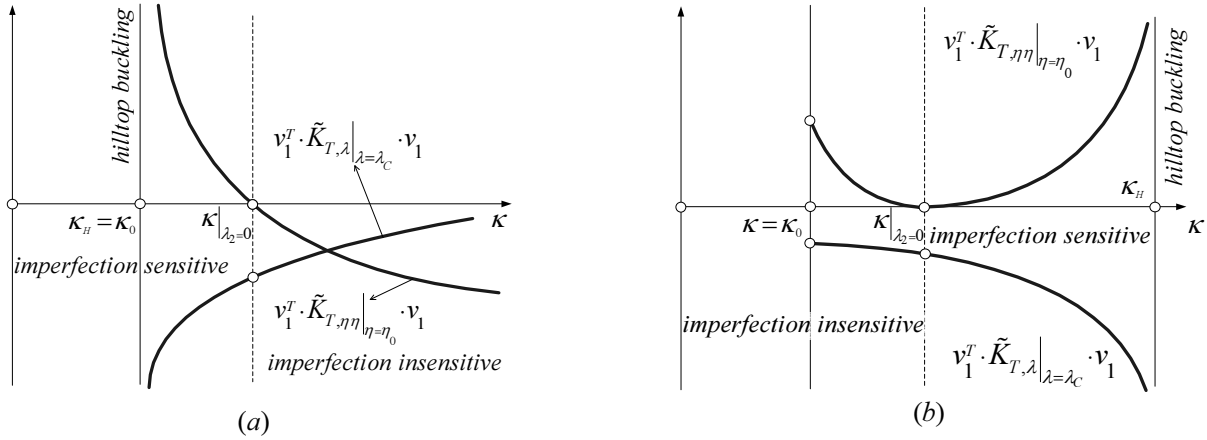

Fig. 2. Hilltop buckling as (a) the A and (b) the Ω of sensitivity analysis

$$b_2 = \infty^1,\ d_3 = \infty^2,\quad -\infty < \lambda_4 < 0. \tag{59}$$

Eq. (59) corroborates the conjecture that for symmetric bifurcation at the hilltop all coefficients with an even subscript in the asymptotic series expansion (4) must be negative, finite numbers.

6. Classification of sensitivity analyses of the initial postbuckling behavior

6.1. Consistently linearized eigenvalue problem

With the help of the consistently linearized eigenvalue problem, sensitivity analyses of the initial postbuckling behavior can be categorized in two classes. For a specific value of κ, this eigenproblem is defined as (Helnwein 1997; Mang, Helnwein 1995):

$$\left[\tilde{\boldsymbol{K}}_T + (\lambda^* - \lambda)\tilde{\boldsymbol{K}}_{T,\lambda}\right]\cdot \boldsymbol{v}^* = \boldsymbol{0}. \tag{60}$$

In (60), $(\lambda^* - \lambda) \in \mathbb{R}$ is the eigenvalue corresponding to the eigenvector $\boldsymbol{v}^* \in \mathbb{R}^N$. Because of (20), λ^* and $\boldsymbol{v}^*$ are functions of λ. If $\lambda^* = \lambda$, $\tilde{\boldsymbol{K}}_T$ is singular. Thus, a candidate for the stability limit is found (Helnwein 1997). The first eigenpair of (60) is $\left(\lambda_1^*,\ \boldsymbol{v}_1^*\right)$. At the stability limit,

$$\lambda_1^* = \lambda = \lambda_C,\quad \boldsymbol{v}_1^* = \boldsymbol{v}_1. \tag{61}$$

(Recall that λ_C and $\boldsymbol{v}_1$ appear on the right-hand side of (4) and (5), respectively.)

Furthermore, at the stability limit (Mang *et al.* 2006),

$$\boldsymbol{v}_{1,\lambda}^* = a_1\boldsymbol{v}_1 \quad \wedge$$

$$\boldsymbol{v}_{1,\lambda\lambda}^* = 3\left(a_1^2 + a_1^*\right)\boldsymbol{v}_1 + \sum_{j=2}^{N} \frac{\boldsymbol{v}_j^{*T}\cdot\tilde{\boldsymbol{K}}_{T,\lambda\lambda}\cdot\boldsymbol{v}_1}{(\lambda_1^* - \lambda_j^*)(\boldsymbol{v}_j^{*T}\cdot\tilde{\boldsymbol{K}}_{T,\lambda}\cdot\boldsymbol{v}_j^*)}\,\boldsymbol{v}_j^*. \tag{62}$$

Equating (47) to (16) gives

$$\lambda_2 = -\frac{a_1}{\boldsymbol{v}_1^T\cdot\tilde{\boldsymbol{K}}_{T,\lambda\lambda}\cdot\boldsymbol{v}_1}\boldsymbol{v}_1^T\cdot\tilde{\boldsymbol{K}}_{T,\eta\eta}\cdot\boldsymbol{v}_1, \tag{63}$$

where (Mang *et al.* 2006)

$$a_1 = -\frac{1}{2}\lambda_{1,\lambda\lambda}^*\Big|_{\lambda=\lambda_C}. \tag{64}$$

Because $\boldsymbol{v}_1^T\cdot\tilde{\boldsymbol{K}}_{T,\lambda}\cdot\boldsymbol{v}_1$ does not vanish (Mang *et al.* 2006), the same applies to $a_1 / \boldsymbol{v}_1^T\cdot\tilde{\boldsymbol{K}}_{T,\lambda\lambda}\cdot\boldsymbol{v}_1$, as follows from (16). Consequently, $a_1 = 0$ requires $\boldsymbol{v}_1^T\cdot\tilde{\boldsymbol{K}}_{T,\lambda\lambda}\cdot\boldsymbol{v}_1 = 0$. It follows that

$$\frac{a_1}{\left(\boldsymbol{v}_1^T\cdot\tilde{\boldsymbol{K}}_{T,\lambda\lambda}\cdot\boldsymbol{v}_1\right)\Big|_{\lambda=\lambda_C}} = -\frac{1}{2}\frac{\lambda_{1,\lambda\lambda}^*}{\boldsymbol{v}_1^{*T}\cdot\tilde{\boldsymbol{K}}_{T,\lambda\lambda}\cdot\boldsymbol{v}_1^*}\Bigg|_{\lambda=\lambda_C} = \frac{0}{0} =$$

$$= -\frac{1}{2}\frac{\lambda_{1,\lambda\lambda\lambda}^*}{\left(2\boldsymbol{v}_1^{*T}\cdot\tilde{\boldsymbol{K}}_{T,\lambda\lambda}\cdot\boldsymbol{v}_{1,\lambda}^* + \boldsymbol{v}_1^{*T}\cdot\tilde{\boldsymbol{K}}_{T,\lambda\lambda\lambda}\cdot\boldsymbol{v}_1^*\right)}\Bigg|_{\lambda=\lambda_C} = \tag{65}$$

$$= \frac{3a_1^*}{\boldsymbol{v}_1^T\cdot\tilde{\boldsymbol{K}}_{T,\lambda\lambda\lambda}\cdot\boldsymbol{v}_1} \neq 0,$$

where use of (19), (61.1) and (62.1) with $a_1 = 0$ was made and, following from (65),

$$a_1^* = -\frac{1}{6}\lambda_{1,\lambda\lambda\lambda}^*\Big|_{\lambda=\lambda_C}. \tag{66}$$

For class II, in contrast to class I, $a_1 = 0$ implies

$$a_1^* = 0 \tag{67}$$

which requires

$$\boldsymbol{v}_1^T\cdot\tilde{\boldsymbol{K}}_{T,\lambda\lambda\lambda}\cdot\boldsymbol{v}_1 = 0, \tag{68}$$

as follows from (65). Thus

$$\frac{a_1^*}{\boldsymbol{v}_1^T\cdot\tilde{\boldsymbol{K}}_{T,\lambda\lambda\lambda}\cdot\boldsymbol{v}_1} = \frac{\lambda_{1,\lambda\lambda\lambda}^*}{\left(2\boldsymbol{v}_1^{*T}\cdot\tilde{\boldsymbol{K}}_{T,\lambda\lambda}\cdot\boldsymbol{v}_{1,\lambda}^* + \boldsymbol{v}_1^{*T}\cdot\tilde{\boldsymbol{K}}_{T,\lambda\lambda\lambda}\cdot\boldsymbol{v}_1^*\right)\Big|_{\lambda=\lambda_C}} =$$

$$= \frac{0}{0} = -\frac{1}{6}\frac{\lambda_{1,\lambda\lambda\lambda\lambda}^*}{\left(2\boldsymbol{v}_{1,\lambda}^{*T}\cdot\tilde{\boldsymbol{K}}_{T,\lambda\lambda}\cdot\boldsymbol{v}_{1,\lambda}^* + 4\boldsymbol{v}_1^{*T}\cdot\tilde{\boldsymbol{K}}_{T,\lambda\lambda\lambda}\cdot\boldsymbol{v}_{1,\lambda}^*\right.}\cdots \tag{69}$$

$$\cdots\frac{}{\left.+2\boldsymbol{v}_1^{*T}\cdot\tilde{\boldsymbol{K}}_{T,\lambda\lambda}\cdot\boldsymbol{v}_{1,\lambda\lambda}^* + \boldsymbol{v}_1^{*T}\cdot\tilde{\boldsymbol{K}}_{T,\lambda\lambda\lambda\lambda}\cdot\boldsymbol{v}_1^*\right)\Big|_{\lambda=\lambda_C}} =$$

$$= -\frac{1}{6}\frac{\lambda_{1,\lambda\lambda\lambda\lambda}^*}{\left(2\boldsymbol{v}_1^{*T}\cdot\tilde{\boldsymbol{K}}_{T,\lambda\lambda}\cdot\boldsymbol{v}_{1,\lambda\lambda}^* + \boldsymbol{v}_1^{*T}\cdot\tilde{\boldsymbol{K}}_{T,\lambda\lambda\lambda\lambda}\cdot\boldsymbol{v}_1^*\right)\Big|_{\lambda=\lambda_C}} \neq 0.$$

For the special case of

$$\tilde{\boldsymbol{K}}_{T,\lambda\lambda}\cdot\boldsymbol{v}_1 = \boldsymbol{0}, \tag{70}$$

$$\frac{a_1^*}{\boldsymbol{v}_1^T\cdot\tilde{\boldsymbol{K}}_{T,\lambda\lambda\lambda}\cdot\boldsymbol{v}_1} = -\frac{1}{6}\frac{\lambda_{1,\lambda\lambda\lambda\lambda}^*}{\boldsymbol{v}_1^{*T}\cdot\tilde{\boldsymbol{K}}_{T,\lambda\lambda\lambda\lambda}\cdot\boldsymbol{v}_1^*}\Bigg|_{\lambda=\lambda_C} \neq 0. \tag{71}$$

The joint vanishing of a_1 and a_1^* represents a limiting case insofar as it correlates with a limiting value of $\lambda_2 (a_1 = 0)$. (See Sections 6.2. and 6.3.)

6.2. Class I

This class is characterized by

$$\boldsymbol{v}_j^{*T}\cdot\tilde{\boldsymbol{K}}_{T,\lambda\lambda}\cdot\boldsymbol{v}_1 = 0 \quad \forall\ j \in \{2,3,\ldots,N\}, \tag{72}$$

resulting in

$$\boldsymbol{v}_{1,\lambda\lambda}^* = 3(a_1^2 + a_1^*)\boldsymbol{v}_1. \tag{73}$$

This remarkable orthogonality relation represents the special case that the curve described by the vector function $\boldsymbol{v}_1^*(\lambda)$ degenerates into a straight line.
For

$$\lambda_2 = 0, \tag{74}$$

$$a_1 < 0,\quad b_2 > 0,\quad \lambda_4 = d_3. \tag{75}$$

The signs of a_1 and b_2 are the same as for hilltop buckling. The sign of $\lambda_4 = d_3$ which follows from (28) is indeterminate. For

$$a_1 = 0, \tag{76}$$

$$\lambda_2 > 0. \tag{77}$$

For class I, (76) requires (Steinboeck *et al.* 2008a)

$$\tilde{\boldsymbol{K}}_{T,\lambda\lambda}\cdot\boldsymbol{v}_1 = \boldsymbol{0}. \tag{78}$$

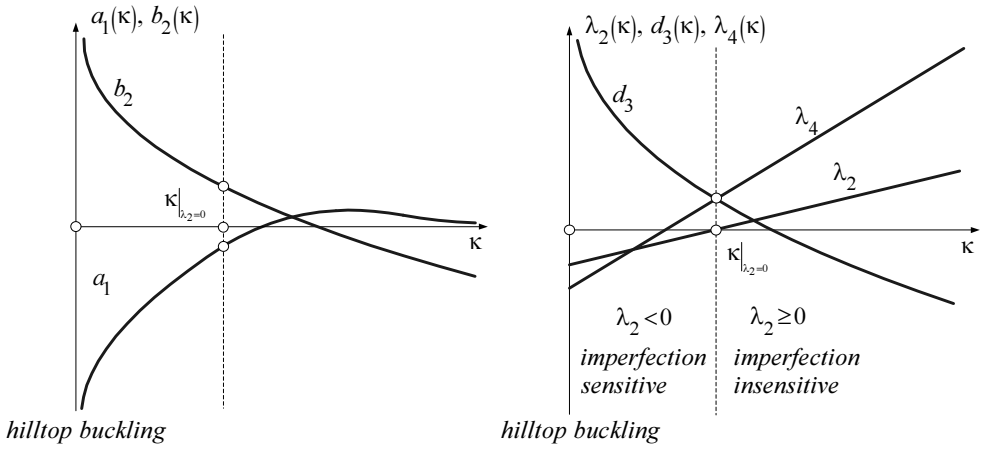

Fig. 3. Sensitivity analysis (class I, hilltop buckling as the starting point):
(*a*) $a_1(\kappa), b_2(\kappa)$; (*b*) $\lambda_2(\kappa), d_3(\kappa), \lambda_4(\kappa)$

Fig. 3a, b shows qualitative plots of a_1 and b_2 (λ_2, d_3, and λ_4) as functions of κ which denotes the stiffness of an elastic spring attached to the structure, details of which will be given in Chapter 7 (Numerical investigation).

Fig. 3 refers to a situation where hilltop buckling represents the starting point of sensitivity analysis, characterized by

$$\kappa = 0. \tag{79}$$

In Fig. 3b,

$$d_3(\lambda_2 = 0) = \lambda_4(\lambda_2 = 0) > 0\,, \tag{80}$$

indicating that at $\lambda_2 = 0$ the structure is already imperfection insensitive. For $d_3(\lambda_2 = 0) < 0$, the structure would still be imperfection sensitive at $\lambda_2 = 0$. For $d_3(\lambda_2 = 0) = 0$, the sign of $\lambda_6(\lambda_2 = 0, \lambda_4 = 0)$ would determine the initial postbuckling state of the structure. The linear dependence of λ_2 and λ_4 on κ represents a special situation.

6.3. Class II

In this class, (72) does not hold. Furthermore, contrary to class I,

$$\lambda_2 = 0 \tag{81}$$

jointly occurs with

$$a_1 = 0 \quad (\text{with } \tilde{\boldsymbol{K}}_{T,\lambda\lambda} \cdot \boldsymbol{v}_1 \neq \boldsymbol{0} \vee = \boldsymbol{0}) \tag{82}$$

and

$$a_1^* = 0 \quad (\text{with } \tilde{\boldsymbol{K}}_{T,\lambda\lambda\lambda} \cdot \boldsymbol{v}_1 \neq \boldsymbol{0}\,). \tag{83}$$

Substitution of (82) into (62.1) and of (82) and (83) into (62.2) gives

$$\boldsymbol{v}_{1,\lambda}^* = \boldsymbol{0} \quad \wedge$$

$$\boldsymbol{v}_{1,\lambda\lambda}^* = \sum_{j=2}^{N} \frac{\boldsymbol{v}_j^{*T} \cdot \tilde{\boldsymbol{K}}_{T,\lambda\lambda} \cdot \boldsymbol{v}_1}{\left(\lambda_1^* - \lambda_j^*\right)\left(\boldsymbol{v}_j^{*T} \cdot \tilde{\boldsymbol{K}}_{T,\lambda} \cdot \boldsymbol{v}_j^*\right)} \boldsymbol{v}_j^* \begin{cases} = \boldsymbol{0} & \text{if } \tilde{\boldsymbol{K}}_{T,\lambda\lambda} \cdot \boldsymbol{v}_1 = \boldsymbol{0} \\ \neq \boldsymbol{0} & \text{else} \end{cases} \tag{84}$$

indicating a singular point $\boldsymbol{v}_1^*(\lambda_C) = \boldsymbol{v}_1$ in the form of a cusp on the curve described by the vector function $\boldsymbol{v}_1^*(\lambda)$.

Fig. 4a(b) shows qualitative plots of a_1 and b_2 (λ_2, d_3, and λ_4) as functions of κ which denotes the stiffness of an elastic spring attached to the structure, details of which will be given in Chapter 7 (Numerical investigation). Fig. 4 refers to a situation where hilltop buckling represents the starting point of sensitivity analysis, characterized by

$$\kappa = 0\,. \tag{85}$$

Substitution of (81) into (28) and into its first derivative with respect to κ gives,

$$(d_3 - \lambda_4) \quad = 0\,, \tag{86}$$

$$b_2 \quad \lambda_{2,\kappa} + (d_3 - \lambda_4)_{,\kappa} \quad = 0\,. \tag{87}$$

Because of (82) and, contrary to Figure 3(a), of $\lim_{\kappa\to\infty} a_1 \neq 0$ (Fig. 4a),

$$b_2 = 0 \quad \wedge \quad \left(d_3 - \lambda_4\right)_{,\kappa} = 0 \tag{88}$$

(Fig. 4, 5). According to Fig. 4b,

$$d_3(\lambda_2 = 0) = \lambda_4(\lambda_2 = 0) < 0\,, \tag{89}$$

indicating that for $\lambda_2 = 0$ the structure is still imperfection sensitive.

Following from (88.2)

$$d_{3,\kappa}(\lambda_2 = 0) = \lambda_{4,\kappa}(\lambda_2 = 0) \tag{90}$$

(Fig. 4b, and 5b). Fig. 4 is based on $\boldsymbol{v}_{1,\lambda\lambda}^* \neq \boldsymbol{0}$.

Fig. 5a(b) shows qualitative plots of a_1 and b_2 (λ_2, d_3, and λ_4) as functions of κ standing for the thickness of the structure, details of which will be given in Chapter 7 (Numerical investigation). The initial value of κ is denoted as κ_0. The curves illustrate a situation where hilltop buckling represents the end of sensitivity analysis because snap-through would become relevant to loss of stability if κ was further increased.

If $\boldsymbol{v}_{1,\lambda\lambda}^* = \boldsymbol{0}$, then also (Fig. 5b)

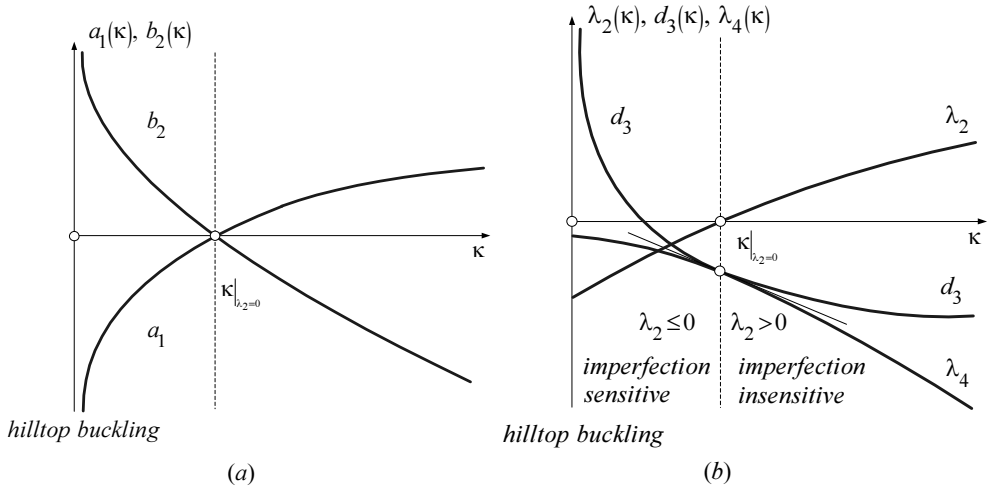

Fig. 4. Sensitivity analysis (class II, hilltop buckling as the starting point):
(*a*) $a_1(\kappa)$, $b_2(\kappa)$; (*b*) $\lambda_2(\kappa)$, $d_3(\kappa)$, $\lambda_4(\kappa)$

$$\lambda_{2,\kappa}(\lambda_2 = 0) = 0. \tag{91}$$

Furthermore, (86) and (88.2) disintegrate into (Fig. 5b)

$$d_3(\lambda_2 = 0) = \lambda_4(\lambda_2 = 0) = 0 \quad \wedge$$
$$d_{3,\kappa}(\lambda_2 = 0) = \lambda_{4,\kappa}(\lambda_2 = 0) = 0. \tag{92}$$

Substitution of (81), (82), (88.1), and (91) into the second derivative of (28) with respect to κ yields (Fig. 5b)

$$d_{3,\kappa\kappa}(\lambda_2 = 0) = \lambda_{4,\kappa\kappa}(\lambda_2 = 0) = 0. \tag{93}$$

At $\lambda_2 = 0$, there is no conversion from imperfection sensitivity into imperfection insensitivity. $\lambda_2 = 0$ marks the starting point of deterioration of the initial postbuckling behavior accompanied by continued improvement of the prebuckling behavior.

7. Numerical examples

The numerical investigation consists of one example each for the two classes of sensitivity analyses of the initial postbuckling behavior. In the example for class I (II), hilltop buckling is chosen as the starting point (end) of such sensitivity analysis. The example for class I (II) is solved analytically (numerically by the FEM).

7.1. Example for class I

Fig. 6 shows a planar, static, conservative system with two degrees of freedom. The description of this system closely follows (Steinboeck *et al.* 2008a) where additional details can be found. Both rigid bars, ① and ② have the same length L and in the non-buckled state they are in-line. The bars are linked at one end and supported by turning-and-sliding joints at their other ends. A horizontal linear elastic spring of stiffness k and a vertical linear elastic spring of stiffness κk are attached to turning-and-sliding joints. A spring of stiffness μk "pulls" the two bars back into their in-line position. The system is loaded by a vertical load λP at the vertical turning-and-sliding joint. The two displacement coordinates are the angles u_1 and u_2, summarized in the vector $\boldsymbol{u} = [u_1, u_2]^T$. In order to write the out-of-balance force $\boldsymbol{G}$ in the structure as defined in (1), other coordinates

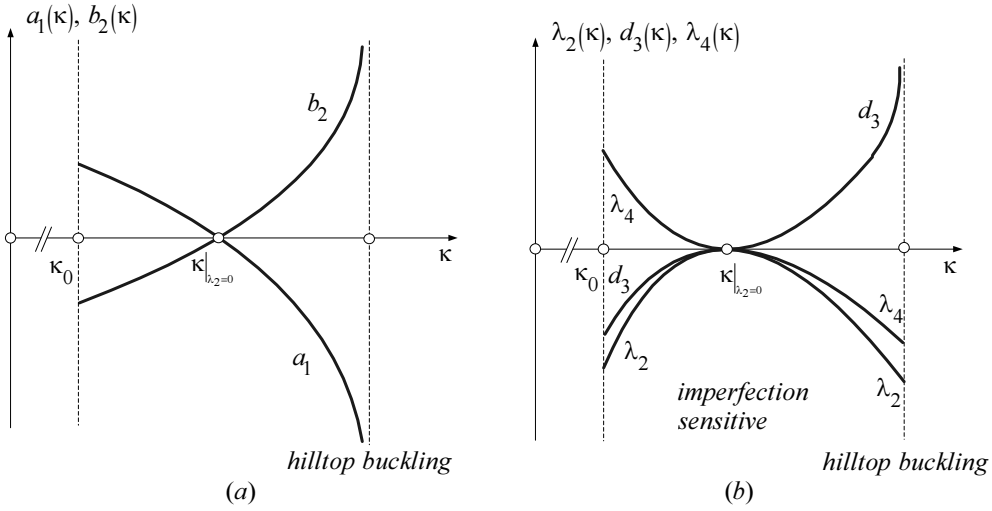

Fig. 5. Sensitivity analysis (class II, hilltop buckling as the end):
(*a*) $a_1(\kappa)$, $b_2(\kappa)$; (*b*) $\lambda_2(\kappa)$, $d_3(\kappa)$, $\lambda_4(\kappa)$

would have to be chosen. In fact, the angle u_1 would have to be replaced by the vertical position of the upper turning-and-sliding joint. This would only require a simple coordinate transformation. For convenience, however, the angle u_1 was chosen as a coordinate. The unloaded position, delineated in gray, is defined by $\boldsymbol{u} = [\boldsymbol{u}_{10}, 0]^T$. This system was first investigated in (Schranz *et al.* 2006) and later on in (Steinboeck *et al.* 2008).

The potential energy expression follows as

$$\begin{aligned} V(\boldsymbol{u},\lambda) &= 2\kappa k L^2 \left(\sin(u_{10}) - \sin(u_1)\cos(u_2)\right)^2 \\ &+ \frac{\mu k}{2} L^2 \sin^2(u_2) \\ &+ 2 k L^2 \left(\cos(u_{10}) - \cos(u_1)\cos(u_2)\right)^2 \\ &- \lambda P 2 L \left(\sin(u_{10}) - \sin(u_1)\cos(u_2)\right). \end{aligned} \tag{94}$$

The equilibrium equations $V_{,u_1} = 0$ and $V_{,u_2} = 0$ are satisfied for the primary path

$$\begin{aligned} &u_2 = 0, \\ &\lambda = \frac{2Lk}{P}\left((1-\kappa)\sin(u_1) - \cos(u_{10})\tan(u_1) + \kappa\sin(u_{10})\right), \end{aligned} \tag{95}$$

and for the secondary path

$$\begin{aligned} u_2 &= \pm \arccos\left(\frac{4}{4-\mu}\frac{\cos(u_{10})}{\cos(u_1)}\right), \\ \lambda &= \frac{2Lk}{P}\left(\frac{\mu - 4\kappa}{4-\mu}\cos(u_{10})\tan(u_1) + \kappa\sin(u_{10})\right). \end{aligned} \tag{96}$$

Since a perfect system is assumed, the sign of u_2 is indeterminate, i.e. it is not known into which direction the two bars will buckle. The tangent-stiffness matrix follows as

$$\tilde{\boldsymbol{K}}_T = 4kL^2\, diag \begin{Bmatrix} \kappa\left(1 + \sin(u_{10})\sin(u_1) - 2\sin^2(u_1)\right) \\ +1 + \cos(u_{10})\cos(u_1) - 2\cos^2(u_1) \\ -\lambda\dfrac{P}{2kL}\sin(u_1); \end{Bmatrix}$$

$$\begin{Bmatrix} \kappa\left(\sin(u_{10})\sin(u_1) - \sin^2(u_1)\right) \\ +\cos(u_{10})\cos(u_1) - \cos^2(u_1) \\ -\lambda\dfrac{P}{2kL}\sin(u_1) \end{Bmatrix}. \tag{97}$$

Its derivative with respect to λ can be computed by

$$\tilde{\boldsymbol{K}}_{T,\lambda} = V_{,\boldsymbol{uuu}} \cdot \tilde{\boldsymbol{u}}_{,\lambda} + \frac{\partial V_{,\boldsymbol{uu}}}{\partial \lambda}, \tag{98}$$

where $\tilde{\boldsymbol{u}}_{,\lambda}$ is the derivative of the displacement vector along the primary path, which can be determined from the linear equation

$$\tilde{\boldsymbol{G}}_{,\lambda} = \tilde{\boldsymbol{K}}_T \cdot \tilde{\boldsymbol{u}}_{,\lambda} + \frac{\partial \tilde{\boldsymbol{G}}}{\partial \lambda} = \boldsymbol{0}. \tag{99}$$

The expression for $\tilde{\boldsymbol{K}}_{T,\lambda}$ looks similar to (97). For the sake of conciseness, it has been omitted. Hence, all terms necessary for solving the eigenproblem (60) are available.

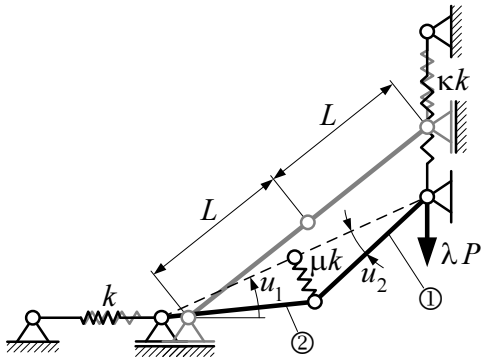

Fig. 6. Pin-jointed two-bar system (Steinboeck *et al.* 2008a)

$u_{10} \in (-\pi/2, \pi/2)$, $\mu \in \mathbb{R}^+$ and $\kappa \in \mathbb{R}^+$ are parameters that can be varied in order to achieve qualitative changes of the system. However, in this work, only κ was modified. The remaining two parameters were taken as $\mu = 3/5$ and $u_{10} = 0.67026$, in which case hilltop buckling occurs for $\kappa = 0$ representing the starting point of sensitivity analysis of the buckling load and the initial postbuckling behavior. The load-displacement path for hilltop buckling and its projection onto the plane $u_2 = 0$ are shown in Figs 7a and 7b, respectively. S labels the unloaded state. As the load is increased, the state will move up along the primary path until $C = D$ is reached. In case of a load-controlled system, snap-through will occur. However, a displacement-controlled system would bifurcate and the state would traverse one branch of the secondary path.

If $\eta = u_2$, the relevant coefficients of the series expansion (4) generally follow as

$$\begin{aligned} &\lambda_1 = 0, \qquad \lambda_2 = \frac{k\,L}{P}\frac{(\kappa - \mu/4)}{\sqrt{1 - \dfrac{\cos^2(u_{10})}{(1-\mu/4)^2}}}, \\ &\lambda_3 = 0, \qquad \lambda_4 = -\frac{\lambda_2}{12}\frac{1 - 4\dfrac{\cos^2(u_{10})}{(1-\mu/4)^2}}{1 - \dfrac{\cos^2(u_{10})}{(1-\mu/4)^2}}. \end{aligned} \tag{100}$$

Thus, $\lambda_4 \propto \lambda_2$. For $\kappa = 0$ (hilltop buckling), this system is imperfection sensitive ($\lambda_2 < 0$), and λ_C exceeds the ultimate load of any imperfect system. Increasing the parameter κ, i.e. the stiffness of the vertical spring, improves the postbuckling behavior insofar as λ_2 eventually begins increasing monotonically. The system is imperfection insensitive for $\kappa > \mu/4$. Fig. 7c refers to the transition case $\kappa = \mu/4$. Remarkably, $\lambda = \lambda_C$ holds along the whole postbuckling path, which requires

$$\lambda_i = 0 \quad \forall \in \mathbb{N} \setminus \{0\}. \tag{101}$$

This situation is referred to as zero-stiffness postbuckling. In contrast to the present example, where zero-stiffness postbuckling is a special case of symmetric bifurcation, it may also be a special case of antisymmetric bifurcation

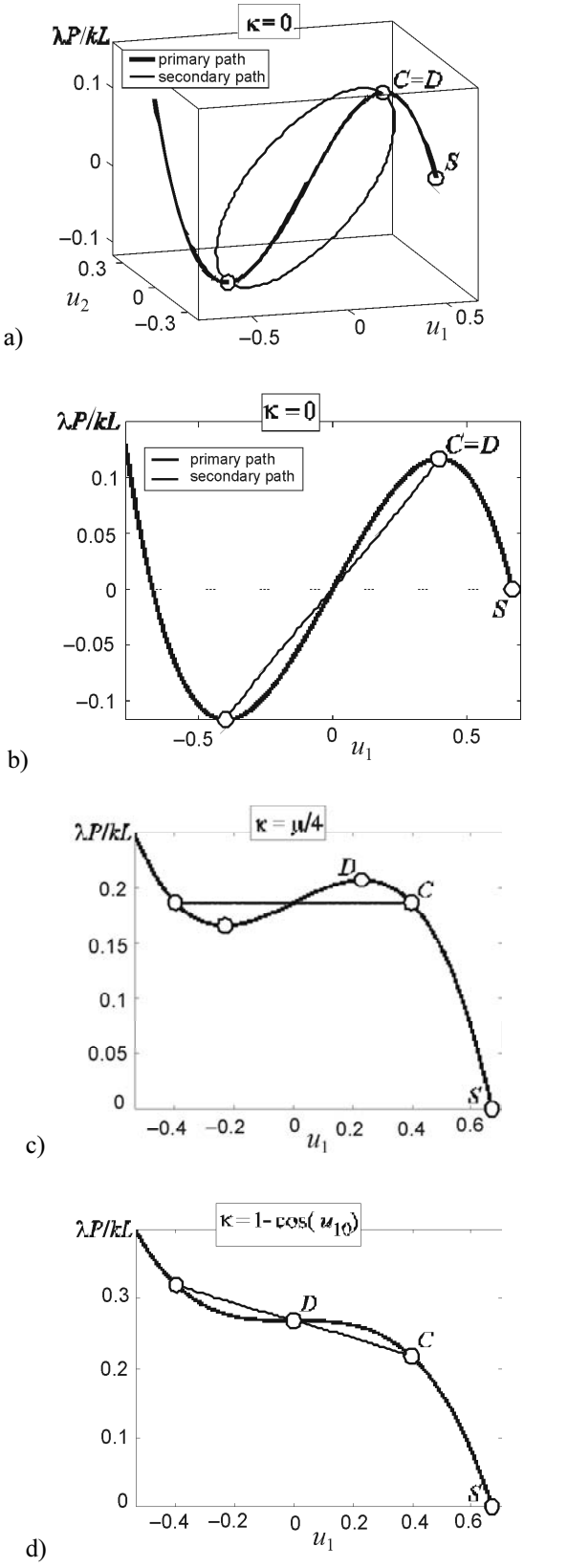

Fig. 7. Selected results from sensitivity analysis of the initial postbuckling behavior of the pin-jointed two-bar system shown in Fig. 5: (a) load-displacement path for hilltop buckling; (b), (c), (d) projections of load-displacement paths onto the plane $u_2 = 0$ for hilltop buckling, zero-stiffness postbuckling, and the beginning of monotonically increasing prebuckling paths

(Steinboeck *et al.* 2008). However, this special case is of little practical interest because it does not represent a transition from imperfection sensitivity to imperfection insensitivity.

As κ is further increased, the critical displacement at the beginning of monotonically increasing prebuckling paths approaches 0. Eventually, at $\kappa = 1 - \cos(u_{10})$, the two turning points meet at $\boldsymbol{u} = \mathbf{0}$, where the primary path exhibits a saddle point D. This situation is shown in Fig. 7d. A comparison of Fig. 7b, c, d shows that the bifurcation point C is increasing less strongly with increasing κ than the snap-through point D. Hence, the two points are diverging from each other.

7.2. Example for class II

Fig. 8 shows a shallow cylindrical shell subjected to a point load at the center. It contains the geometric data as well as values for the modulus of elasticity E and the shear modulus G. The reference load $\bar{P} = 1000$ kN is scaled by a dimensionless load factor λ. The description of sensitivity analysis of the initial postbuckling behavior of the shell is based on (Schranz *et al.* 2006) where this structure was previously investigated and where additional details can be found.

In contrast to the first example, Koiter's initial postbuckling analysis was not used to compute post- buckling paths for this example. Instead of it, prebuckling and postbuckling analyses were performed by means of the FEM, using the finite element program MSC.Marc (MCS.MARC 2005).

The parameter κ that is varied in the course of sensitivity analysis of the initial postbuckling behavior of the shell is the thickness. The initial value κ_0 was chosen as 5.35 cm. Load-displacement paths for $\kappa = 5.35$ cm, 6.35 cm, 7.35 cm, and 8.10 cm are shown in the left part of Fig. 9 where u denotes the displacement of the load point. The right part of Fig. 9 contains details of corresponding plots of the left part.

For each one of the four values of κ considered, the structure is imperfection sensitive. For the thinnest shell ($\kappa = 5.35$ cm), the slope of the postbuckling path at the stability limit is negative whereas the curvature is positive. The postbuckling path has a minimum followed by a maximum. For the second thinnest shell ($\kappa = 6.35$ cm), the slope of the postbuckling path at the stability limit is approximately zero, i.e. $\lambda_2 \approx 0$.

According to Fig. 5b, for $\lambda_2 = 0$, also $\lambda_{2,\kappa} = 0$, $\lambda_4 = 0$, $\lambda_{4,\kappa} = 0$, and $\lambda_{4,\kappa\kappa} = 0$. Because of the negative curvature of the postbuckling path at the stability limit, the first non-vanishing coefficient of (4), which because of symmetric bifurcation must have an even subscript, is negative. For the second thickest shell ($\kappa = 7.35$ cm) and the thickest shell ($\kappa = 8.10$ cm), both the slope and the curvature of the postbuckling path are negative at the stability limit. For the thickest shell, hilltop buckling occurs. It represents the end of sensitivity analysis of the initial postbuckling behavior of the shell, because loss of

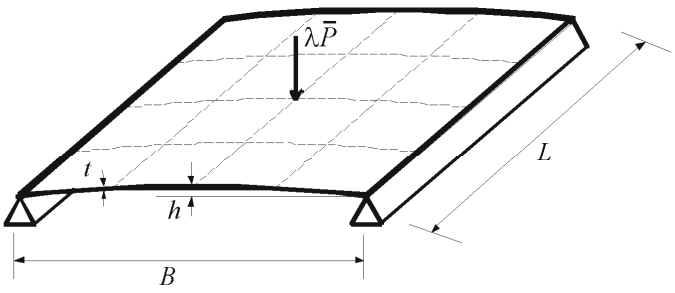

Fig. 8. Shallow cylindrical shell subjected to a point load at the center (Schranz *et al.* 2006)

stability would occur by snap-through if the thickness of the structure was further increased.

A comparison of the plots in Fig. 9 shows that the bifurcation point C is increasing more strongly with increasing κ than the snap-through point D. Hence, the two points are converging to each other. This comparison also shows that $\lambda_2 = 0$ marks the starting point of deterioration of the initial postbuckling behavior accompanied by continued improvement of the pre- buckling behavior, characterized by

$$d\lambda_2 < 0 \quad \wedge \quad d\kappa > 0\,. \tag{102}$$

Fig. 9 elucidates that the increase of the thickness of the shell does not result in a transition from imperfection sensitivity to imperfection insensitivity.

8. Conclusions

- It was shown that hilltop buckling is imperfection sensitive.
- It is conjectured that for symmetric bifurcation all non-vanishing coefficients in the asymptotic series expansion for the load level at an arbitrary point of the secondary path (see (4)) are negative, i.e. $\lambda_{2k} < 0\ \forall\, k \in \mathbb{N}\setminus\{0\}$. This conjecture is based on a hypothesis representing the generalization of a scheme that was validated numerically for the special case of λ_4 (see (58)). Verification of this conjecture is planned.
- Hilltop buckling as the starting point – the A – of sensitivity analysis of the initial postbuckling behavior of elastic structures is characterized by $\lambda_{2,\kappa} > 0$, with $d\lambda_2 > 0 \wedge d\kappa > 0$, where κ is a design parameter that is increased in the course of the analysis. It marks the starting point of an improvement of the initial postbuckling behavior of the structure, accompanied by an improvement of the prebuckling behavior. The bifurcation point and the snap-through point are diverging from each other.
- Hilltop buckling as the end – the Ω – of such sensitivity analysis is characterized by $\lambda_{2,\kappa} < 0$, with $d\lambda_2 < 0 \wedge d\kappa > 0$. It is preceded by a deterioration of the initial postbuckling behavior of the structure, accompanied by an improvement of the prebuckling behavior. Hilltop buckling represents the end of sensitivity analysis because snap-through would become relevant to loss of stability if κ was further increased. The bifurcation point and the snap-through point are converging to each other.
- Two classes of sensitivity analyses of the initial postbuckling behavior of elastic structures were identified. Class I is characterized by a remarkable orthogonality condition derived from the so-called consistently linearized eigenproblem (see (60)). It may be viewed as a special case of class II for which this condition does not hold. In mechanical terms, for the first class the decisive eigenvector of the eigenproblem, $\boldsymbol{v}_1^*(\lambda)$, describes a rectilinear motion, with λ representing the time. For class II, however, $\boldsymbol{v}_1^*(\lambda)$ describes a general motion. Hence, it is conjectured that class I is restricted to relatively simple problems.
- The two classes of sensitivity analyses determine the mode of conversion of an originally imperfection-sensitive into an imperfection-insensitive structure. Such a conversion is the true motivation for this type of sensitivity analyses.
- For class I, there is no restriction on the sign of $\lambda_4(\lambda_2 = 0)$. Hence, for $\lambda_2 = 0$, the structure may either be already imperfection insensitive or still imperfection sensitive. As a special case, zero- stiffness postbuckling may occur (Fig. 7b).
- For class II, if $\boldsymbol{v}_{1,\lambda\lambda}^*(\lambda_C) \neq \boldsymbol{0}$, then $\lambda_{2,\kappa}(\lambda_2 = 0) > 0$, and $\lambda_4(\lambda_2 = 0) < 0$ (see Fig. 4(b)), but if $\boldsymbol{v}_{1,\lambda\lambda}^*(\lambda_C) = \boldsymbol{0}$, then $\lambda_{2,\kappa}(\lambda_2 = 0) = 0$, $\lambda_4(\lambda_2 = 0) = 0$, and $\lambda_{4,\kappa}(\lambda_2 = 0) = 0$, $\lambda_{4,\kappa\kappa}(\lambda_2 = 0) = 0$ (Fig. 5b). For the second case there is no transition from imperfection sensitivity into imperfection insensitivity. Thus, the increase of the thickness of a structure, while improving its prebuckling behavior, does not result in such a transition. For class II, $\lambda_2 = 0$ correlates with a singular point in form of a cusp on the curve described by the vector function $\boldsymbol{v}_1^*(\lambda)$ at the point $\boldsymbol{v}_1^*(\lambda_C) = \boldsymbol{v}_1$ (see (84)). The type of the cusp depends on whether or not $\boldsymbol{v}_{1,\lambda\lambda}^*(\lambda_C)$ is zero.
- The present investigation is viewed as a step in the direction of better understanding the reasons for the initial postbuckling behavior of a particular elastic structure and of its interplay with the prebuckling

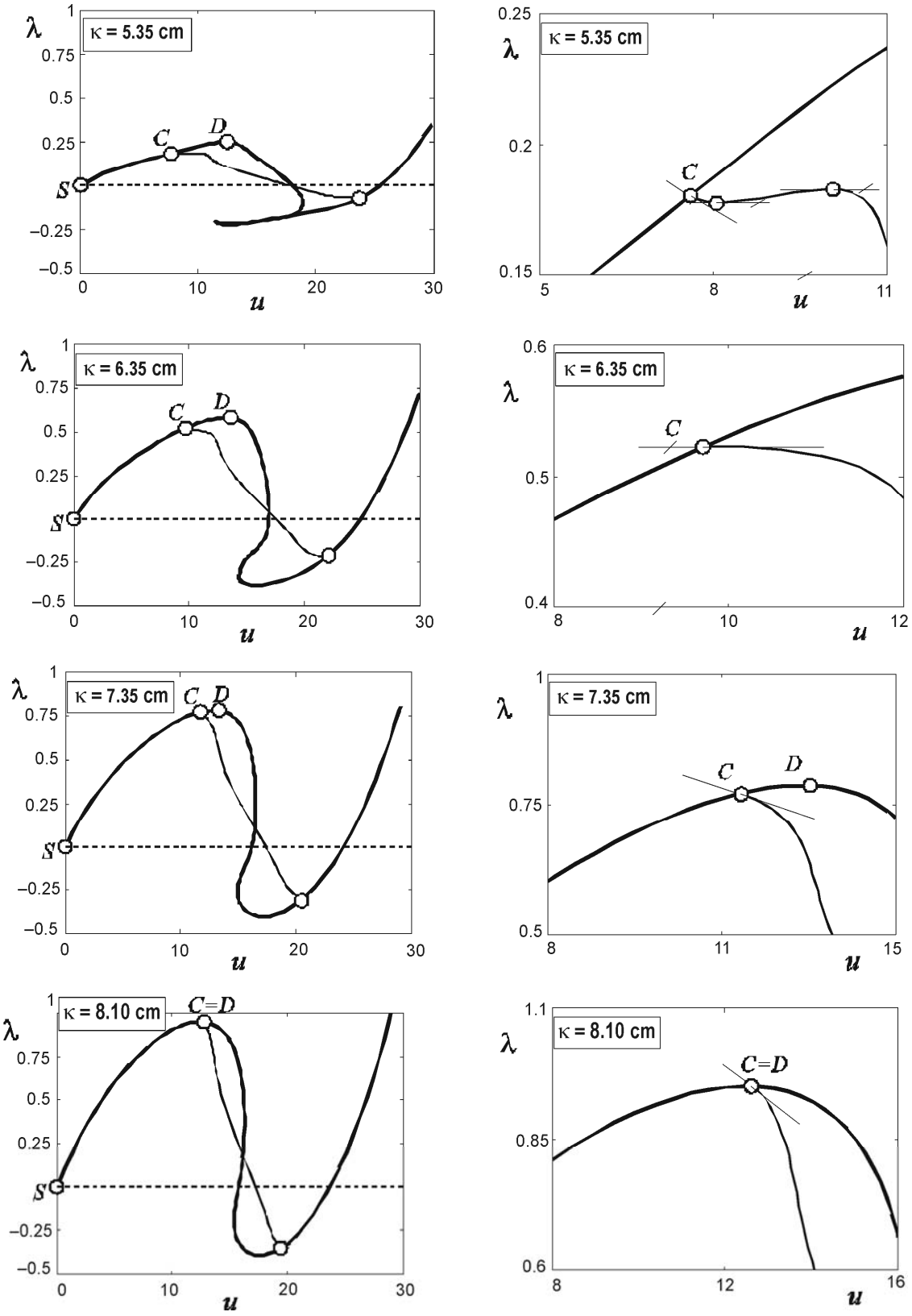

(a) (b)

Fig. 9. Selected results from sensitivity analysis of the initial postbuckling behavior of the shallow cylindrical shell shown in Fig. 7: (a) Load-displacement paths for different values of the thickness of the shell, with the largest value referring to hilltop buckling; (b) details of load-displacement paths

behavior. Such understanding will help to avoid the design of structures with unfavorable postbuckling characteristics. In this sense, the present study is aimed at changing the widespread opinion about postbuckling as a structural feature that can hardly be influenced.

Acknowledgements

The junior authors thankfully acknowledge financial support of the Austrian Academy of Sciences.

References

Bochenek, B. 2003. Problems of structural optimization for post-buckling behaviour, *Struct. Multidisciplinary Optim.* 25/5–6: 423–435.

Fujii, F.; Noguchi, H. 2002. Multiple hill-top branching, in *Proc. 2nd Int. Conf. on Structural Stability and Dynamics*, World Scientific, Singapore.

Helnwein, P. 1997. *Zur initialen Abschätzbarkeit von Stabilitätsgrenzen auf nichtlinearen Last-Verschiebungspfaden elastischer Strukturen mittels der Methode der Finiten Elemente* [On ab initio assessability of stability limits on nonlinear load-displacement paths of elastic structures by means of the finite element method]: Ph.D. Thesis, Vienna University of Technology, Österreichischer Kunst- und Kulturverlag, Vienna.

Koiter, W. 1967. On the stability of elastic equilibrium, Translation of 'Over de Stabiliteit van het Elastisch Evenwicht' (1945), in *NASA TT F-10833*, Polytechnic Institute Delft, H. J. Paris Publisher: Amsterdam.

Mang, H. A.; Helnwein, P. 1995. Second-order a-priori estimates of bifurcation points on geometrically nonlinear prebuckling paths, in *Proc. Int. Conf. of Computational Engineering Science*, Hawaii, USA. Springer, Berlin, II: 1511–1516.

Mang, H. A.; Schranz, C.; Mackenzie-Helnwein, P. 2006. Conversion from imperfection-sensitive into imperfection-insensitive elastic structures I: Theory, *Comput. Methods Appl. Mech. Engrg.* 195: 1422–1457.

MSC.MARC volume A: 2005. *Theory and user information*, *MSC.Marc manuals*, 145–152.

Ohsaki, M.; Ikeda, K. 2006. Imperfection sensitivity analysis of hill-top branching points with many symmetric bifurcation points, *International Journal of Solids and Structures* 43: 4704–4719.

Schranz, C.; Krenn, B.; Mang, H. A. 2006. Conversion from imperfection-sensitive into imperfection-insensitive elastic structures II: Numerical investigation, *Comput. Methods Appl. Mech. Engrg.* 195: 1458–1479.

Steinboeck, A.; Jia X. Hoefinger, G.; Mang, H. A. 2008a. Remarkable postbuckling paths analyzed by means of the consistently linearized eigenproblem, *Int. J. Numer. Meth. Engng.* 76: 156–182.

Steinboeck, A.; Jia X.; Hoefinger, G.; Mang, H. A. 2008b. Conditions for symmetric, antisymmetric, and zero-stiffness bifurcation in view of imperfection sensitivity and insensitivity, *Comput. Methods Appl. Mech. Engrg.* 197: 3623–3636.

AUKŠTESNYSIS KLUPUMAS, KAIP A IR Ω TAMPRIŲJŲ KONSTRUKCIJŲ ELGSENOS UŽ PRADINIO KLUPUMO RIBOS JAUTRUMO ANALIZĖJE

H. A. Mang, X. Jia, G. Hoefinger

Santrauka

Nagrinėjant apkraunamos konstrukcijos elgseną, bifurkacijos taško sutapdinimas su staigaus pasikeitimo tašku vadinamas aukštesniuoju klupumu. Šiame straipsnyje šis taškas yra arba pradžios taškas A, arba proceso pabaigos taškas Ω. Šie taškai imami atliekant tampriųjų konstrukcijų elgsenos jautrumo analizę už pradinio suklupimo ribos. Parodyta, kad aukštesnysis konstrukcijos klupumas priklauso nuo jos geometrinių netikslumų. Kai aukštesniojo klupumo jautrumo analizė sutapdinama su pradiniu tašku, bifurkacijos taškas ir staigaus pasikeitimo taškas artėja vienas prie kito. Identifikuojamos dvi jautrumo analizės klasės sprendžiant nuoseklaus linearizavimo savųjų reikšmių uždavinį. Uždavinio sprendinys lemia daugiau ar mažiau efektyvią klupumo formą, kuri leidžia pakeisti pradinę netikslumams jautrią konstrukciją į konstrukciją, nejautrią jiems. Skaitiniai tyrimai patvirtina teorinius rezultatus. Šie tyrimai padeda nustatant įvairias klupumo formas, nagrinėjant tampriųjų konstrukcijų elgseną už pradinio klupumo ribos ir ryšį su jos elgsena prieš šią ribą.

Reikšminiai žodžiai: nuoseklaus linearizavimo savųjų reikšmių uždavinys, aukštesnysis klupumas, (ne)jautrumas netikslumams, Koiterio analizė už pradinės klupumo ribos, simetrinė bifurkacija, nulinio standumo elgsena už klupumo ribos.

Herbert A. MANG is a Professor of Strength of Materials and Head of the Institute for Mechanics of Materials and Structures of Vienna University of Technology (VUT). He was Dean of the Department of Civil Engineering and Prorector of VUT. He is a Full Member of the Austrian Academy of Sciences (AAS) and a Member of 16 Foreign Academies of Sciences or Engineering. He was Secretary General and President of the AAS. His main research interests are mechanics of deformable solids, structural mechanics, computational mechanics, computational acoustics, multi-physics and multi-scale analyses. He has co-authored or co-edited 18 books and published more than 400 articles on these subjects.

Xin JIA is a PhD student at the Institute for Mechanics of Materials and Structures of Vienna University of Technology. His research interests include solid and structural mechanics and nonlinear finite element methods with special emphasis on analysis techniques for the solution of problems of structural stability.

Gerhard HÖFINGER is a PhD student in Professor Mang's group at the Institute for Mechanics of Materials and Structures of Vienna University of Technology. He got his Master's degree in mathematics from the same university. His research interests include structural mechanics, finite elements and mathematical modeling and simulation.